Published in final edited form as:
Brain Res. 2008 August 21; 1226: 39–55. doi:10.1016/j.brainres.2008.05.082.

Colocalization of caldesmon and calponin with cortical afferents, metabotropic glutamate and neurotrophic receptors in the lateral and central nuclei of the amygdala

Khristofor Agassandian and **Martin D. Cassell**
Department of Anatomy & Cell Biology, University of Iowa, Iowa City, IA 52242, USA

Abstract

Caldesmon (Cd) and calponin (Cp) are two actin/calmodulin-binding proteins involved in 'actin-linked' regulation of smooth muscle and non-muscle Mg^{2+} actin-activated myosin II ATPase activity. However, in the brain, Cd and Cp are associated with the regulation of the neuronal cytoskeleton. In this study we investigated the subcellular distribution of Cd and Cp in the amygdala and their possible relationship to metabotropic glutamate (mGluR1α and 5) and TrkB receptors which interact with inputs from the cortex and are involved in associative learning. Cd and Cp immunoreactivity (IR) was mainly found in dendritic spines, along dendritic microtubules, and in neuronal perikarya but never in axon terminals. Punctate labeling representing spine labeling was restricted to small patches in the lateral nucleus of amygdala, intercalated cell masses (ICM), and the lateral subdivision of central nucleus. This restricted distribution may reflect local afferent activation. In addition, Cd, Cp, mGluR1α and cortical afferents are co-distributed in the ICM distributed in the lateral nucleus and lateral capsular division of the central nucleus, and the lateral division of the central nucleus itself. Consistent with our previous studies, TrkB IR in the central nucleus was associated with Cd and Cp immunoreactive spines whereas mGluR1α IR and mGluR5 IR were almost exclusively associated with the PSDs of asymmetric synapses, in most cases apposed by cortical terminals. mGluR1α and TrkB immunoreactivities were invariably associated with each other. Overall, these findings suggest that caldesmon and calponin in the amygdala are closely associated with afferents and receptors that have been strongly implicated in associative learning.

Keywords

learning; memory; amygdala; Ca^{2+}-binding proteins; TrkB; mGluR1/5

1. INTRODUCTION

Current models of how the amygdala mediates classical conditioning of a neutral stimulus (CS) to an aversive stimulus (US) focus heavily on the role of the lateral nucleus (LeDoux, 2000; Radley et al., 2007). In these models, partial overlap of cue-relevant cortical and thalamic inputs in the lateral nucleus (LA) is thought to provide the interaction necessary for CS-US association (Mahanty and Sah, 1999; Rosenkranz and Groce, 2002). Establishment of the ability of the CS

Corresponding author: Dr. Khristofor Agassandian, The University of Iowa, Dept. of Anatomy and Cell Biology, 51, Newton Rd, BSB, Iowa City, IA 52245, USA, Tel: (319) 335-6838, Fax: (319) 335-7198, E-mail: khristofor-agassandian@uiowa.edu.

to acquire and elicit the responses characteristic of the US is believed to occur through pre- and post-synaptic changes in neurons of the LA (Maren, 2005; Rogan et al., 1997; Tsvetkov et al., 2002). The principle post-synaptic changes so far identified in LA neurons involve activation of metabotropic glutamate receptors (Fendt and Schmid, 2002), changes in intracellular calcium stores (Power and Sah, 2007) and increases in phophorylated Ca^{2+}/calmodulin-dependent protein kinase II (Rodrigues et al., 2004), translocation of the actin-binding protein profilin to dendritic spines (Lamprecht et al., 2006) and increases in spinophilin-immunoreactive spines (Radley et al., 2006).

While spinophilin and profilin may be useful markers for dendritic spines in the amygdala, changes in spine numbers associated with learning have to be detected against a background of dendritic spines that are normally immunoreactive for spinophilin or profilin. A potentially more useful marker of dendritic spine re-organization would be one that appears only in spines actively in the process of forming or changing shape. Large, actin-dependent conformational changes in dendritic spines occur over periods of seconds to a few minutes e.g. (Fischer et al., 1998) and stabilization of spines is directly related to the influx of calcium through voltage-gated channels e.g. (Fischer et al., 2000). Potential candidates for markers of active, short-term dendritic plasticity in the amygdala could be the calcium-modulated actin-binding proteins caldesmon and calponin, both of which have been shown to be involved in spine re-modeling (Ferhat et al., 2003). Caldesmon and calponin are present on the post-synaptic side of symmetric synapses and accumulate in post-synaptic densities (PSDs) of asymmetric synapses in rat hippocampus (Agassandian et al., 2000). Cd and Cp in dendritic spines (DS) appear to bind to actin and Ca^{2+}-calmodulin, and stimulate the polymerization and bundling of actin filaments (Sabatini et al., 2001). Calponin, in fact, has been demonstrated to dramatically increase during spine re-modelling in the hippocampus (Ferhat et al., 2003). The distribution of Cd and Cp in the amygdala is not known.

Group 1 metabotropic glutamate receptors (mGluR1 and 5) in the lateral amygdala appear to play a critical role in the establishment of conditioned fear (Fendt and Schmid, 2002). However, immunocytochemical and mRNA detection studies indicate that high levels mGluR1 and mGluR5 are present in the CE (Martin et al., 1992; Shigemoto et al., 1992; Shigemoto et al., 1993). The role of the Group 1 metabotropic receptors in long term potentiation appears to be mediated via increasing levels of intracellular Ca^{2+}, facilitating Ca^{2+} release from internal stores, and regulating Ca^{2+} influx via voltage sensitive Ca^{2+}-channels (Riedel and Reymann, 1996). Group 1 metabotropic receptors and calponin and caldesmon could thus provide an important link between cue-related inputs and actin-mediated remodelling of dendritic spines in the amygdala during learning.

We have previously demonstrated that terminals containing brain derived neurotrophic factor (BDNF) end on dendritic spines in CeL and the neurotrophic receptor TrkB is present in CE neurons and is apposed to cortical terminals (Agassandian et al., 2006). In the hippocampus, BDNF appears to be heavily involved in regulating F-actin polymerization which is critical to the stabilization of dendritic spines and the consolidation of long term potentiation (Kramar et al., 2006; Rex et al., 2007). A similar process may occur in the central nucleus though a link between BDNF, TrkB, cortical inputs and actin has yet to be made.

In summary, the present study sought i) to examine the regional and subcellular localization of Cd and Cp in the amygdala; ii) to determine whether and where Cd and Cp in the amygdala, in particular the lateral and central nuclei, are co-distributed with learning-related afferents and metabotropic glutamate receptors, and; iii) to determine the cellular interrelationships between Cd, Cp, mGluR1/5 and TrkB receptors. Parts of this work have appeared in abstract form (Agassandian and Cassell, 2006).

2. RESULTS

Light Microscopy

A general low level of Cd and Cp immunoreactivity in the neuropil was observed in all subdivisions of the amygdala but the overall appearance was of considerable regional variations in staining intensity (Fig. 1A, Fig. 2A). The densest neuropil staining, the majority of neurons labeled by both antibodies, and some punctuate staining, were concentrated in CE and the lateral part of the LA (Fig. 1B, Fig. 2B). In the CE, most Cd- or Cp-immunoreactive neurons were found in CeL though approximately 50% of CeL neurons showed very little or no immunoreactivity (Fig. 1B,C; Fig. 2B, C). Neuronal labeling appeared to be primarily perikaryal (though immunolabeled proximal dendrites were consistently seen) with many cells also showing what appeared to be nuclear labeling. Patches of punctate staining were observed along the lateral and dorsal edges of CeL. These patches were seen in every case though their extent and location varied slightly between cases. In all cases, the punctate labeling was associated with a concentration of immuno-labeled cells (Fig.1B and C; 2B and C). The lateral capsular region (CeLC) between the CE and basolateral amygdala containing the main intercalated cell masses (ICM) also contained immunoreactive neurons, mostly in the small cluster at the dorsolateral corner of CeL (Fig.1C; Fig.2 C) but also in the other, more ventrally situated clusters. Punctate labeling was also present in these clusters. In Cd-immunostained sections, a patch of immunoreactive neurons associated with punctate labeling was seen in the dorsomedial aspect of CeLC, close to the ventral globus pallidus. The lateral and basolateral nuclei contained less by about half the number of labeled neurons found in the CE. These neurons were sparsely scattered throughout the lateral nucleus except for a concentration along its lateral border with the external capsule in the ventrolateral division. In this division, a dense patch of neuropil and punctate staining was consistently seen (Fig.1B and Fig.2B). In BL, Cd and Cp immunoreactive neurons were mostly restricted to the posterior division (BLP) and along the junction with the deep layer of the periamygdaloid cortex. The anterior basolateral division was almost completely devoid of Cd/Cp immunoreactivity. The specificity of Cd and Cp immunoreactivity was confirmed by eliminating the primary antibody and pre-adsorbing the antibody with the appropriate antigen (Cd or Cp). Both eliminated all staining in the brain (Fig. 1D and Fig. 2D).

After BDA injection into the dysgranular posterior insular cortex (Fig. 3A) labeled axons and terminals were almost completely restricted to CeL and the dorsolateral part of LA (Fig. 3B), consistent with previous studies (Shi and Cassell, 1998). BDA injections into dorsal perirhinal cortex (Fig.3C) resulted in labeled terminals in the dorsolateral LA and dorsal CeLC, but not CeL (Fig.3D).

Immunolabelling of mGluR1α and mGluR5 presented largely as fine-grain punctate labeling and was distributed throughout the amygdala with the densest labeling in the lateral and central nuclei (Fig. 3E and F). Immunolabeling for mGlurR1α and mGlurR5 in the LA was restricted to the lateral portion (Fig.3E and F), consistent with previous studies (Rodrigues et al., 2002). Both antibodies gave a patch-like staining pattern in the CE but subtle differences were observed. Immunostaining for mGluR1α was heaviest in CeL, in the small intercalated cell masses in the lateral capsular division of the CE, and in the ventrolateral part of LA (Fig. 3E). The labeling pattern was very similar to that reported for D1 receptors (Fuxe et al., 2003) and GABAergic neurons (Marowsky et al., 2005). The punctate labeling of mGluR5 was likewise concentrated in CeL, dorsolateral LA, and the intercalated clusters, though several small clusters stained by the mGluR1α antibody were not stained (Fig. 3F). There was a distinctly denser distribution of mGluR5 immunoreaction product over the dorsal extension of the lateral capsular division (CeLC), and a prominent cell cluster subjacent to the ventral globus pallidus was heavily stained (Fig.3F).

Overlap composites (Fig. 4E) confirmed that Cd, Cp (Fig.4A), mGluR1α (Fig.4B) and mGluR5, and cortical terminals from the insular (Fig.4C) and Te3/perirhinal cortex (Fig.4D) are heavily concentrated and co-distributed in only three areas: the lateral LA, the ICM in the lateral capsular division of the CE, and in CeL (Fig. 4E).

Electron microscopy

Ultrastructurally, Cd and Cp immunoreactivity demonstrated similar subcellular distribution patterns. Reaction product was found in perikarya, dendrites and dendritic spines (DS) of LA and CE neurons (Fig.5, Fig.6, and Fig.7) but never in terminals. In both amygdalar regions, reaction product was primarily identified in perikaryal cytoplasm with many neurons exhibiting reaction product in the nucleus (Fig. 5A and C, Fig. 6A, Fig. 7A and B). Immunoreactive neurons were frequently found adjacent to unlabeled neurons (Figs.5C) and glia (Fig. 7B).

Cd and Cp immunoreactivity in dendrites was not widely observed, particularly in the LA, but was generally characterized by densely packed reaction product associated with microtubules and post-synaptic densities (PSDs) (Fig. 5D, Fig. 6B, Fig. 7D and F). Most Cd and Cp immunoreactivity appeared associated with dendritic spines (Fig. 5E, Fig. 6B, Fig. 7E) Dendritic spines, regardless of the immunolabeling of the parent dendrite, consistently showed strong Cd or Cp IR in their cytoplasm and PSDs (Fig. 5B and Fig. 6B). In the absence of immunolabeling of terminals, it is very likely that the punctate staining seen under light microscopy reflects immunolabeling of dendritic spines in both LA and CE. Though only seen when a longitudinally cut dendrite was encountered, Cd/Cp immunoreactive spines were observed immediately adjacent to unlabeled spines on the same dendrite (Fig. 5B). In these instances, Cd/Cp immunoreactivity was also associated with a bundle of filamentous elements in the portion of the parent dendrite subjacent to the immunoreactive spine (e.g. Fig.5B).

The most common type of interaction between Cd or Cp immunoreactive structures and (unlabeled) axon terminals was an asymmetric synapse (Fig. 5D and E, Fig. 6B, Fig. 7C, D and E) though some dendrites containing IR in their cytoplasm also made symmetric synaptic contacts with terminals (Fig. 5F and Fig. 7F). Occasionally, symmetric synapses were marked by accumulation of Cd or Cp IR along their postsynaptic membranes. In no instance was Cd or Cp IR observed in presynaptic membranes.

TrkB post-embedding immunogold immunocytochemistry was combined with pre-embedding Cd or Cp immunocytochemistry to determine their inter-relationship. Our previous report (Agassandian et al., 2006) using pre-embedding immunocytochemistry for TrkB receptor detection identified immunoreactivity primarily in association with post-synaptic membranes of CE neurons though occasional immunoreactive terminals were observed. Here, 39% of gold particles in a sampled area (128 sq. μm) were over or within 50nM of Cd or Cp immunoreactive post-synaptic densities (e.g. Fig. 8A to F; Fig. 9A to F) and 60.1% of gold particles in the same sample were associated with dendritic profiles that were immunoreactive for Cd or Cp. This comparable pattern found using the same antibody but two different immunochemical methods strongly suggests that the greater part of the gold particle distribution reflects antibody binding to antigenic sites associated with TrkB receptors. Cd/Cp and TrkB relationships fell into three different categories depending on the presence of TrkB IR in dendrites, DSs and axon terminals: TrkB IR in Cd or Cp positive dendrites and DSs as well as in axon terminals synapsing with these structures (Figs. 8A and D); TrkB immunoreactive and Cd or Cp immuno-positive dendrites and spines synapsing with TrkB negative axon terminals (Fig. 8 B,C, and F, and Fig. 9C, D and E); TrkB negative, but Cd or Cp positive dendrites and DSs contacting with TrkB positive terminals (Fig. 8E and 9F).

Cortical terminals and metabotropic glutamate receptors

Pre-embedding immunolabeling of mGluR1α and mGluR5 receptors in both LA and CE presented almost exclusively as electron-dense reaction product associated with post-synaptic densities on dendritic spines (Fig.9A and Fig.10A, B) and dendritic shafts (Fig. 9B and Fig. 10C,D). In most cases, immunopositive dendrites showed mGluR1α IR *only* in PSDs though other mGluR1α-positive dendrites also had IR associated with microtubules. mGLUR5 immunoreactivity was also primarily associated with post-synaptic densities on dendritic shafts and spines though immunoreactivity was rarely seen outside of the membrane. This is consistent with previous ultrastructural studies of metabotropic glutamate receptors in the amygdala (e.g. Rodrigues et al., 2002). In the CE, axon terminals labeled by BDA injections into the insular cortex made exclusively asymmetric synaptic contacts with dendritic spines and dendrites (Fig. 9A and B; Fig. 10A–D) in the CE consistent with previous reports (Sun et al., 1994). Where a clear synaptic contact was evident, in almost every case BDA labeled terminals were apposed to a mGluR immunoreactive PSD. In a sample of micrographs of the CE from two cases (128 sq.μM total area), 66.7% of identifiable BDA-labeled terminals were in apposition to mGluR1α immunoreactivity associated with PSDs. For mGluR5 immunostained sections, sample micrographs (covering a total of 202 sq.μM) from the CE (2 cases) showed 70.2% of BDA-labeled terminals apposed to PSDs with mGluR5 immunoreactivity.

TrkB post-embedding immunocytochemistry was performed on sections containing contacts between BDA labeled cortical terminals and mGluR1α positive dendrites and DSs. The distribution of gold particles was identical to that found when Trk-B immunoreactivity was detected by post-embedding immunocytochemistry on Cd/Cp immunoreactive structures (Figs. 8). Similarly, we found that TrkB IR was present on both contacting structures: BDA-labeled axon terminals and mGluR1α immunoreactive dendrites or spines (Fig. 9C, and D). In addition, TrkB-positive and BDA labeled axon terminals were occasionally observed contacting TrkB-negative and mGluR1α-positive dendrites and spines (Fig. 9D, F). The most frequent contact observed, however, was a BDA labeled axon terminal forming a synapse with a TrkB and mGluR1α immunoreactive dendrite or spine (Fig. 9C, D).

Finally, pre-embedding immunocytochemistry for BDA-labeled cortical terminals/mGluR5 was combined with post-embedding immunocytochemistry for Cd and Cp (Fig.10). In a random sample of electron micrographs (covering 328 sq.μm in total) from the CE, 79.8% of gold particles were associated with dendritic profiles (only 1.9% with terminals) for Cp immunostained material and 72.5% of gold particles with dendritic profiles (3.2% with terminals) for Cd-immunostained material. This is consistent with the predominantly dendritic labeling seen with pre-embedding immunocytochemistry. Around a third of dendritic profiles immunoreactive for Cd (29.2%) and Cp (34.1%) contained mGluR5 immunoreactivity (Fig. 10) and over half of these had BDA-labeled cortical terminals forming synaptic contacts with dendritic spines (Fig.10A and B) and shafts (Fig.10A and B).

3. DISCUSSION

This study provides the first description of the cellular distribution of caldesmon and calponin in the amygdala and their association with neural elements potentially involved in synaptic plasticity related to associative learning. Our findings provide morphological evidence for i) the restriction of Cd and Cp to perikarya and dendritic spines of a limited number of neurons and in a limited number of amygdaloid nuclei; ii) interactions between these Ca^{2+}/actin-modulating proteins, cortical inputs and three important receptors, Trk-B, mGluR1α and mGluR5, known to be involved in synaptic plasticity and the processes of learning and memory; iii) co-distribution of Cd, Cp, cortical terminals and metabotropic glutamate receptors not only

in the lateral divisions of the lateral nucleus of the amygdala but also in the intercalated cell clusters in the capsular and lateral divisions of the central nucleus (Fig. 4E).

Characteristics of Cd and Cp in the amygdala

Light and electron microscopic examination of Cd and Cp immunoreactivity in the amygdala indicate a similar restricted distribution of these proteins both in terms of their localization to specific amygdaloid nuclei and their subcellular distribution. Caldesmon and calponin are clearly present in neurons in the lateral and central nuclei but in a limited number and concentrated in specific sub-areas. In the lateral nucleus, Cd/Cp neurons are scattered throughout but tend to be concentrated in the lateral part adjacent to the external capsule whereas in the CE they were almost all located in CeL and the intercalated cell masses (ICM) in CeLC. Though we did not co-stain LA, CeL or the ICM for Cd/Cp and GABA, these regions all contain aggregations of GABA-ergic, medium-sized spiny neurons (Sun and Cassell, 1993; Marowsky et al., 2005) so it is possible that these proteins are associated only with this particular class of neuron. Medium-sized spiny neurons in CeL can be categorized on the basis of peptide content (Cassell and Gray, 1989; Day et al., 1999) and as Cd/Cp was not seen in all neurons they may be associated with a particular subclass of CeL neurons.

As reported in the cerebellum (Represa et al., 1995) and hippocampus (Agassandian et al., 2000), both proteins in the amygdala are most abundant in dendritic spines but much less concentrated in dendritic shafts and absent from terminal boutons. This subcellular distribution pattern is very similar to that found for the actin-binding protein spinophilin (Muly et al., 2004; Ouimet et al., 2004) and may, in part, reflect the actin-binding properties of Cd and Cp. Spinophilin is found in dendritic spines throughout the amygdala (Radley et al., 2006), as well as the cerebral cortex, hippocampus, cerebellum and caudate-putamen (Allen et al., 1997; Ouimet et al., 2004), while profilin is present in some 30% of spines in the LA prior to application of conditioning paradigms (Lamprecht et al., 2006). Cd/Cp labeled dendritic spines (represented by punctate labeling under light microscopy) were concentrated in lateral LA, the dorsal intercalated cell masses and the lateral division of the CE, and were not ubiquitously distributed. However, in these areas, large numbers of unlabeled spines were also present and, moreover, there was a clear dissociation between punctate labeling and neuronal labeling: punctate labeling, i.e. spine labeling, was always associated with clusters of labeled neurons while other clusters of Cd/Cp immunoreactive neurons had no local punctate labeling. This suggests that Cd/Cp in dendritic spines may be there as a result of a purely local event such as afferent or receptor activation rather than being normally present in spines. Neurons in the dorsolateral LA show short latency responses to auditory conditioning stimuli in Pavlovian learning paradigms (Repa et al., 2001) and learning-related ERK/MAP kinase expression (Schafe et al., 2000). The presence of Cd and Cp in spines in the LA, and possibly the CE, may reflect translocation in response to presentation of sensory stimuli.

Alternatively, the presence of Cd/Cp in a restricted population of spines could be related to more long-term, on-going alterations in the actin cytoskeleton of the spine. In the dentate gyrus, reorganization of afferents and dendritic spines one week after pilocarpine-induced seizures is accompanied by a dramatic increase in calponin immunoreactivity (Ferhat et al., 2003).

Co-distribution of Cd and Cp with afferents and mGluR1

The distribution patterns of mGluR1α and mGluR5 immunoreactivities are similar to those reported previously (Rodrigues et al., 2002). It was evident that these metabotropic glutamate receptors are concentrated in the lateral LA, the intercalated cell masses located in the capsular division of the CE, and the lateral division of the CE (Fig. 3E). Significant co-localization of these two receptors to the same neuron has been reported for the nucleus accumbens and caudate-putamen (Mitrano and Smith, 2007; Valenti et al., 2002). Overlay of images of

metabotropic glutamate receptors, Cd/Cp staining and cortical afferents confirmed that the only areas containing high densities of all these elements are the lateral LA, and the capsular and lateral divisions of the CE. In contrast, the medial CE, both anterior and posterior divisions of the basolateral nucleus, and ventral and medial parts of the lateral nucleus either showed low levels of labeling for all these elements or there was minimal co-localization.

Within the LA, the co-distribution of cortical afferents, metabotropic glutamate receptors and overall Cd/Cp immunostaining is localized to the same circumscribed region along its the lateral edge where punctate (spine) Cd/Cp labeling was observed. This region corresponds to a dense cluster of GABAergic neurons ("lateral paracapsular cells" of Marowsky et al., 2005) with a concentration of D1 and mu-opioid receptors (Fuxe et al., 2003; Jacobsen et al., 2006) and is a key component of the dorsolateral lateral nucleus region critical to learning (LeDoux, 2000). However, an identical co-distribution is present in the ICM in dorsal and lateral parts of the capsular division of the CE (the "medial paracapsular cells of (Marowsky et al., 2005)), and in its large lateral division (CeL). Like the lateral LA, the two CE areas have in common medium-sized, spiny GABAergic neurons (Marowsky et al., 2005; Pare and Smith, 1994; Sun and Cassell, 1993), a dense dopaminergic innervation (Freedman and Cassell, 1994), a concentration of D1 and mu-opioid receptors (Fuxe et al., 2003; Jacobsen et al., 2006), and all are targeted by sensory-related subcortical and thalamic afferents (Bernard et al., 1993; Nakashima et al., 2000). This convergence of factors on a distinctive population of neurons spread throughout the dorsal amygdala, rather than restricted to a single nucleus, suggests there may be a more widespread distribution of sites for associative learning in the amygdala, with differences possibly based on afferent modality.

Receptor interactions in the central nucleus

The localization of membrane-related mGluR1α IR to PSDs in the CE corresponds to findings in the rat (and monkey) nucleus accumbens and caudate-putamen where the mGluR1 family of receptors is almost exclusively found postsynaptically in dendrites and spines (Bonsi et al., 2005; Mitrano and Smith, 2007). Group 1 metabotropic glutamate receptors can increase intracellular Ca^{2+} through release from intracellular stores (Fagni et al., 2000). Co-localization of mGluR1α and mGluR5 with Cp and Cd suggests a relationship between these receptors and the calcium-modulating machinery of CE neurons though more detailed work needs to be done.

It is known that BDNF signaling through the TrkB receptor in the amygdala is required for the acquisition of conditioned fear (Rattiner et al., 2004). BDNF and its receptor TrkB play a critical role in activity-dependent synaptic plasticity (Patterson et al., 1996) and have been implicated as mediators of amygdala-dependent learning and memory (Chhatwal et al., 2006). The presence of TrkB IR in both terminals that synapse with Cd or Cp positive dendrites and in Cd or Cp IR dendrites and DSs themselves indicates that at a minimum neurotrophins essential to learning and memory storage in the central nucleus of amygdala are co-localized in dendritic spines with proteins that form a link with the cytoskeleton.

Interestingly, we found that BDA labeled cortical terminals synapse with dendrites and DSs that are immuno-positive for ***both*** mGluR1α and TrkB receptors. The positioning of mGluR1 and TrkB in PSDs of dendrites and dendritic spines, which receive cortical inputs, indicates that mGluR1s associated with neurotrophins and Ca^{2+}-binding proteins are in a perfect position to effect the plastic changes necessary for permanent presentation of sensory-sensory association.

4. EXPERIMENTAL PROCEDURES

Animals

We performed investigations on 22 adult (300g) male Sprague-Dawley rats (Harlan Laboratories, Indianapolis, IN). All studies adhered to the guidelines for care and use of experimental animals (NIH publications No. 80-23) and were approved by the Animal Care and Use Committee of the University of Iowa.

Anesthesia

All experiments were performed under aseptic conditions. Animals were deeply anesthetized with Nembutal sodium solution (50 mg/kg) administered intraperitoneally.

Caldesmon and Calponin immunocytochemistry

Caldesmon immunoreactivity was detected by using an affinity-purified antibody (Goat anti-Caldesmon (N-19) polyclonal antibody, Santa Cruz Biotechnology, Inc.) directed at a peptide near the N-terminus of human caldesmon. The antibody has been shown by Western blotting to detect both muscular and non-muscular forms of caldesmon of human and rodent origin at approximately 150kDa . Calponin-3 (or acidic calponin), the form of calponin found in brain, was detected using an affinity purified antibody made against a peptide sequence from an internal region of human Calponin-3 (Goat anti-Calponin 3 polyclonal antibody, Santa Cruz Biotechnology, Inc.). Western blotting by manufacturer reported staining of a single band at approximately 39kDa. Pre-adsorption of both antibodies with respective immunizing peptide abolished staining in the brain (Fig.1D and Fig.2D). Caldesmon and calponin immuno-staining in the hippocampus was identical to that reported previously using different well-characterized antibodies to these proteins (Agassandian et al., 2000).

Animals were deeply anesthetized and perfused transcardially with PBS containing 2% paraformaldehyde and 0.5% glutaraldehyde. Brains were removed, post-fixed in the same fixative for 24h and cut using a vibratome into 35–50 μM thick coronal or horizontal sections. Sections were then incubated overnight at 4°C in a 1:200 dilution of primary anti-Caldesmon polyclonal antibody or a 1:400 dilution of primary Goat anti-Calponin polyclonal antibody. Sections were then washed with PBS and placed in 1:200 biotinylated secondary antibody, followed by biotin detection with solutions from an ABC Elite kit (Vector). Visualization was with treatment with a 0.1% solution of 3,3'-diamonobenzidine (DAB) containing 0.03% hydrogen peroxide. For control studies the adjacent sections were processed using the same protocol without primary antibodies or processed with primary antisera (1:200 or 1:400) that was pre-adsorbed with an excess of the immunizing peptide (25–50 μg/ml of antibody). Sections were dehydrated, cleared and cover-slipped. Sections selected for electron microscopic analysis were post-fixed with 1% OsO_4, dehydrated in an acetone/alcohol series, and flat embedded in Mollenhauer Epon-Araldite Formula (Electron Microscopic Sciences). Under 10X magnification, pieces of flat-embedded sections containing the lateral, basolateral and central nuclei of the amygdala were cut out using bevelled cuts to preserve orientation, and mounted on pre-trimmed Epon bullets. Ultrathin sections from were then cut with a Leica ultramicrotome, stained with uranyl acetate and lead citrate, and examined with a Jeol-1230 electron microscope.

Tracer Injections in Insular and Perirhinal cortex

Stereotaxically guided injections of biotinylated dextran amine (BDA) were made into the insular cortex and the dorsal perirhinal cortex. In brief, the skull over the parietal lobe was exposed through an incision in the scalp and a small hole was drilled in the bone. A glass micropipette angled 90° from the horizontal and directed anteriorly was stereotaxically placed

into the targeted cortex. The micropipette was filled with 10% BDA (Vector Laboratories) solution and BDA was iontophoresed for 2 minutes with a 5 μA positive pulse mode current (5 seconds of iontophoresis alternating with 5 second pauses). After iontophoresis, the pipette was left in place for 2–4 minutes and then removed. All wounds were closed and animals were allowed to recover for 5–7 days. Animals were then anesthetized with Nembutal (50 mg/kg) and perfused with 4% paraformaldehyde and 0.5% glutaraldehyde. Brains were removed and cut by vibratome into 35–50 μM thick horizontal sections. For BDA histochemistry, sections were processed with the ABC/DAB technique used for immunocytochemistry.

Metabotropic Glutamate Receptor (mGluR1α and mGluR5) immuno-cytochemistry

Three different antibodies were used to detect metabotropic glutamate receptor immunoreactivity in the amygdala. The mGluR1α receptor was targeted as it is found in medium-sized spiny neurons in the striatum to be apposed to cortical terminals (Testa et al., 1998) and striatal-like medium spiny neurons are found in the CE and intercalated cell masses (Cassell et al., 1999). Two antibodies against peptide sequences in the carboxy end of mGluR1α (AB1551 and AB1595 Chemicon International, Inc) were used initially but as both gave identical patterns only one (AB1551) was used for ultrastructural studies. According to the manufacturer, Western blotting shows this antibody labels a single band at 140kDa. Additional characterization of this particular antibody has been reported, including studies on knock-out mice and transfected cell lines by Mitrano and Smith (2007), who used the antibody to describe mGluR1 immunoreactivity in the nucleus accumbens at the ultrastructural level. No differences in the subcellular distribution of immunoreactivity between that study and the present one were observed. Pre-adsorption of the antibody with the immunizing peptide abolished staining in the brain.

Two polyclonal antibodies (both from Chemicon International, Inc) against mGluR5 were employed though the patterns of immunolabeling in the amygdala were indistinguishable. The first (AB 5675) was raised against the rat receptor, the manufacturer reporting Western blotting giving staining of a single band at approximately 132kDa. The second antibody to mGluR5 was raised against a C-terminus peptide sequence (KSSPKYDTLIIRDYTNSSSSL) from the rat receptor with an added lysine (06–451). Western blotting by the manufacturer showed staining of a single band at approximately 130kDa, and pre-adsorption of the antibody with the immunizing peptide abolished staining in the brain. Mitrano and Smith (2007) employed an antibody from a different manufacturer but to the same sequence to study mGluR5 immunoreactivity in the nucleus accumbens; the subcellular distribution of immunoreactivity reported in that study was essentially identical to that found here. Though cross-reactivity between mGluR1α and mGluR5 antisera was not directly tested, distinct differences in the immunostaining pattern in the amygdala were observed (Fig 3E and F).

All glutamate receptor immunocytochemistry was performed after BDA development. Brain sections were incubated with PBS, blocked with 1% normal; goat serum and incubated in a 1:400 dilution of either anti-metabotropic glutamate receptor-1 or anti-glutamate receptor-5 polyclonal antibodies at 4°C overnight. Sections then were washed with PBS and processed with a 1:200 dilution of secondary antibodies for 2–4 hr. For control studies, adjacent sections were processed as for Cd or Cp immunocytochemistry. For light microscopy, tissue sections were dehydrated, cleared and mounted in Permount. Sections taken for electron microscopic analysis were processed as described above.

Post-embedding immunocytochemical detection of TrkB, calponin and caldesmon

This was performed on ultrathin sections collected on nickel grids. Sections were pretreated with 1% periodic acid followed by 1% sodium metaperiodate, incubated in 5% bovine serum albumin and placed in Goat Anti-TrkB polyclonal antibody (Sigma-Aldrich) or anti-caldesmon

or anti-calponin in TBS overnight at 4°C. The Trk-B antibody was raised against recombinant human Trk-B and the distribution and ultrastructural appearance of immunostaining in the amygdala was reported previously (Agassandian et al., 2006). Pre-adsorption with the immunizing peptide abolished staining at both light and electron microscopic levels. Sections were washed in TBS and placed in 1:10 dilution of colloidal gold Rabbit-Anti-Goat secondary antibody (Aurion) for 1.5 h. Sections were washed with TBS and dH_2O, then stained with uranyl acetate and lead citrate, and examined with a Jeol-1230 electron microscope.

Digital imaging

All light microscopic images were taken by a digital camera (Sciscope Instrument Co) attached to an Nikon Optiphot microscope. To illustrate the locations of areas of overlap between calponin, caldesmon, mGluR1 and cortical terminal fields, sections from the same rostrocaudal level of the amygdala that were processed for one of these four markers were identified. Criteria for matching included the location and size of the stria terminalis and the length of the optic tract. Each section was digitally photographed, converted into a grayscale image which was partitioned into five gray levels where the densest labeling represented by a gray level of 64 (for multiple composites) or 128 (for pairs of images) and no labeling to white (0). Different images were additively combined to give composite images again represented by five gray levels: maximum overlap between different labels was represented by black and no overlap by white. Electron microscopic images were also taken by a Gatan UltraScan 1000 2k×2k CCD digital camera attached to the Jeol-1230 EM.

List of abbreviations

AT, axon terminal
BDNF, brain derived neurotrophic factor
CE, central nucleus of amygdala
CeL, lateral subdivision of central nucleus
CeLC, lateral capsular subdivision of central nucleus
CeM, medial subdivision of central nucleus
Cd, caldesmon
Cp, calponin
D, dendrite
DS, dendritic spine
ICM, intercalated cell masses
DI, dysgranular insular cortex
IR, immunoreactivity
LN, labeled (immunoreactive) neuron
mGluR1, metabotropic glutamate receptor 1
mGluR5, metabotropic glutamate receptor 5
PSD, post-synaptic density
st, stria terminalis
UN, unlabeled (immunonegative) neuron
US, unlabelled spine

Acknowledgments

Funded in part by NIMH grant MH065452.

References Cited

Agassandian C, Plantier M, Fattoum A, Represa A, der Terrossian E. Subcellular distribution of calponin and caldesmon in rat hippocampus. Brain Research 2000;887:444–449. [PubMed: 11134639]

Agassandian K, Cassell MD. Is the subcellular distribution of caldesmon and calponin in rat central nucleus of amygdala involved in synaptic plasticity to support associative learning? Abstracts of Society for Neuroscience Meeting 2006:N134.14.

Agassandian K, Gedney M, Cassell MD. Neurotrophic factors in the central nucleus of amygdala may be organized to provide substrates for associative learning. Brain Research 2006;1076:78–86. [PubMed: 16473337]

Allen PB, Ouimet CC, Greengard P. Spinophilin, a novel protein phosphatase 1 binding protein localized to dendritic spines. Proc. Natl. Acad. Sci. U.S.A 1997;94:9956–9961. [PubMed: 9275233]

Bernard JF, Alden M, Besson JM. The Organization of the Efferent Projections from the Pontine Parabrachial Area to the Amygdaloid Complex - A Phaseolus-Vulgaris Leukoagglutinin (Pha-L) Study in the Rat. J. Comp. Neurol 1993;329:201–229. [PubMed: 8454730]

Bonsi P, Cuomo D, De Persis C, Centonze D, Bernardi G, Calabresi P, Pisani A. Modulatory action of metabotropic glutamate receptor (mGluR) 5 on mGluR1 function in striatal cholinergic interneurons. Neuropharmacology 2005;49:104–113. [PubMed: 16005029]

Cassell MD, Gray TS. Morphology of peptide-immunoreactive neurons in the rat central nucleus of the amygdala. J. Comp. Neurol 1989;281:320–333. [PubMed: 2468696]

Cassell MD, Freedman LJ, Shi CJ. The intrinsic organization of the central extended amygdala. Advancing from the Ventral Striatum to the Extended Amygdala. Ann. NYAS 1999;877:217–241.

Chhatwal JP, Stanek-Rattiner L, Davis M, Ressler KJ. Amygdala BDNF signaling is required for consolidation but not encoding of extinction. Nat.Neurosci 2006:870–872. [PubMed: 16783370]

Day HE, Curran EJ, Watson SJ Jr, Akil H. Distinct neurochemical populations in the rat central nucleus of the amygdala and bed nucleus of the stria terminalis: evidence for their selective activation by interleukin-1beta. J. Comp. Neurol 1999;413:113–128. [PubMed: 10464374]

Fagni L, Chavis P, Ango F, Bockaert J. Complex interactions between mGluRs, intracellular Ca^{2+} stores and ion channels in neurons. Trends Neurosci 2000;23:80–88. [PubMed: 10652549]

Fendt M, Schmid S. Metabotropic glutamate receptors are involved in amygdaloid plasticity. European Journal of Neuroscience 2002;15:1535–1541. [PubMed: 12028364]

Ferhat L, Esclapez M, Represa A, Fattoum A, Shirao T, Ben-Ari Y. Increased levels of acidic calponin during dendritic spine plasticity after pilocarpine-induced seizures. Hippocampus 2003;13:845–858. [PubMed: 14620880]

Fischer M, Kaech S, Knutti D, Matus A. Rapid actin-based plasticity in dendritic spines. Neuron 1998;20:847–854. [PubMed: 9620690]

Fischer M, Kaech S, Wagner U, Brinkhaus H, Matus A. Glutamate receptors regulate actin-based plasticity in dendritic spines. Nat Neurosci 2000;3:887–894. [PubMed: 10966619]

Freedman LJ, Cassell MD. Distribution of dopaminergic fibers in the central division of the extended amygdala of the rat. Brain Research 1994;633:243–252. [PubMed: 7511034]

Fuxe K, Jacobsen KX, Hoistad M, Tinner B, Jansson A, Staines WA, Agnati LF. The dopamine D1 receptor-rich main and paracapsular intercalated nerve cell groups of the rat amygdala: relationship to the dopamine innervation. Neuroscience 2003;119:733–746. [PubMed: 12809694]

Jacobsen KX, Hoistad M, Staines WA, Fuxe K. The distribution of dopamine D1 receptor and mu-opioid receptor 1 receptor immunoreactivities in the amygdala and interstitial nucleus of the posterior limb of the anterior commissure: relationships to tyrosine hydroxylase and opioid peptide terminal systems. Neuroscience 2006;141:2007–2018. [PubMed: 16820264]

Kramar EA, Lin B, Rex CS, Gall CM, Lynch G. Integrin-driven actin polymerization consolidates long-term potentiation. Proc. Natl. Acad. Sci. U.S.A 2006;103:5579–5584. [PubMed: 16567651]

Lamprecht R, Farb CR, Rodrigues SM, Ledoux JE. Fear conditioning drives profilin into amygdala dendritic spines. Nat. Neurosci 2006;9:481–483. [PubMed: 16547510]

LeDoux JE. Emotion Circuits in the Brain. Annual Review of Neuroscience 2000;23:155–184.

Mahanty NK, Sah P. Excitatory synaptic inputs to pyramidal neurons of the lateral amygdala. Eur. J. Neurosci 1999;11:1217–1222. [PubMed: 10103117]

Maren S. Synaptic Mechanisms of Associative Memory in the Amygdala. Neuron 2005;47:783–786. [PubMed: 16157273]

Marowsky A, Yanagawa Y, Obata K, Vogt KE. A specialized subclass of interneurons mediates dopaminergic facilitation of amygdala function. Neuron 2005;48:1025–1037. [PubMed: 16364905]

Martin LJ, Blackstone CD, Huganir RL, Price DL. Cellular localization of a metabotropic glutamate receptor in rat brain. Neuron 1992;9:259–270. [PubMed: 1323311]

Mitrano DA, Smith Y. Comparative analysis of the subcellular and subsynaptic localization of mGluR1a and mGluR5 metabotropic glutamate receptors in the shell and core of the nucleus accumbens in rat and monkey. J. Comp. Neurol 2007;500:788–806. [PubMed: 17154259]

Muly EC, Allen P, Mazloom M, Aranbayeva Z, Greenfield AT, Greengard P. Subcellular distribution of neurabin immunolabeling in primate prefrontal cortex: comparison with spinophilin. Cerebral Cortex 2004;14:1398–1407. [PubMed: 15217898]

Nakashima M, Uemura M, Yasui K, Ozaki HS, Tabata S, Taen A. An anterograde and retrograde tract-tracing study on the projections from the thalamic gustatory area in the rat: distribution of neurons projecting to the insular cortex and amygdaloid complex. Neuroscience Research 2000;36:297–309. [PubMed: 10771108]

Ouimet CC, Katona I, Allen P, Freund TF, Greengard P. Cellular and subcellular distribution of spinophilin, a PP1 regulatory protein that bundles F-actin in dendritic spines. J. Comp. Neurol 2004;479:374–388. [PubMed: 15514983]

Pare D, Smith Y. GABAergic projection from the intercalated cell masses of the amygdale to the basal forebrain in cats. J. Comp. Neurol 1994;344:33–49. [PubMed: 7520456]

Patterson SL, Abel T, Deuel TA, Martin KC, Rose JC, Kandel ER. Recombinant BDNF rescues deficits in basal synaptic transmission and hippocampal LTP in BDNF knockout mice. Neuron 1996;16:1137–1145. [PubMed: 8663990]

Power JM, Sah P. Distribution of IP3-mediated calcium responses and their role in nuclear signalling in rat basolateral amygdala neurons. J. Physiol 2007;580:835–857. [PubMed: 17303640]

Radley JJ, Farb CR, He Y, Janssen WG, Rodrigues SM, Johnson LR, Hof PR, Ledoux JE, Morrison JH. Distribution of NMDA and AMPA receptor subunits at thalamo-amygdaloid dendritic spines. Brain Research 2007;1134:87–94. [PubMed: 17207780]

Radley JJ, Johnson LR, Janssen WG, Martino J, Lamprecht R, Hof PR, Ledoux JE, Morrison JH. Associative Pavlovian conditioning leads to an increase in spinophilin-immunoreactive dendritic spines in the lateral amygdala. Eur. J. Neurosci 2006;24:876–884. [PubMed: 16930415]

Rattiner LM, Davis M, French CT, Ressler KJ. Brain-derived neurotrophic factor and tyrosine kinase receptor B involvement in amygdala-dependent fear conditioning. J. Neurosci 2004;24:4796–4806. [PubMed: 15152040]

Repa JC, Muller J, Apergis J, Desrochers TM, Zhou Y, Ledoux JE. Two different lateral amygdala cell populations contribute to the initiation and storage of memory. Nature Neuroscience 2001;4:724–731.

Represa A, Trabelsi-Terzidis H, Plantier M, Fattoum A, Jorquera I, Agassandian C, Ben-Ari Y, Der Terrossian E. Distribution of caldesmon and of the acidic isoform of calponin in cultured cerebellar neurons and in different regions of the rat brain: an immunofluorescence and confocal microscopy study. Exp. Cell Res 1995;221:333–343. [PubMed: 7493632]

Rex CS, Lin CY, Kramar EA, Chen LY, Gall CM, Lynch G. Brain-derived neurotrophic factor promotes long-term potentiation-related cytoskeletal changes in adult hippocampus. J. Neurosci 2007;27:3017–3029. [PubMed: 17360925]

Riedel G, Reymann KG. Metabotropic glutamate receptors in hippocampal long-term potentiation and learning and memory. Acta Physiol. Scand 1996;157:1–19. [PubMed: 8735650]

Rodrigues SM, Bauer EP, Farb CR, Schafe GE, Ledoux JE. The group I metabotropic glutamate receptor mGluR5 is required for fear memory formation and long-term potentiation in the lateral amygdala. J. Neurosci 2002;22:5219–5229. [PubMed: 12077217]

Rodrigues SM, Farb CR, Bauer EP, Ledoux JE, Schafe GE. Pavlovian fear conditioning regulates Thr286 autophosphorylation of Ca2+/calmodulin-dependent protein kinase II at lateral amygdala synapses. J. Neurosci 2004;24:3281–3288. [PubMed: 15056707]

Rogan MT, Staubli UV, Ledoux JE. Fear conditioning induces associative long-term potentiation in the amygdala. Nature 1997;390:604–607. [PubMed: 9403688]

Rosenkranz JA, Grace AA. Dopamine-mediated modulation of odour-evoked amygdale potentials during pavlovian conditioning. Nature 2002;417:282–287. [PubMed: 12015602]

Sabatini BL, Maravall M, Svoboda K. Ca^{2+} signaling in dendritic spines. Current Opinion in Neurobiology 2001;11:349–356. [PubMed: 11399434]

Schafe GE, Atkins CM, Swank MW, Bauer EP, Sweatt JD, LeDOUX JE. Activation of ERK/MAP Kinase in the Amygdala Is Required for Memory Consolidation of Pavlovian Fear Conditioning. Journal of Neuroscience 2000;20:8177–8187. [PubMed: 11050141]

Shi CJ, Cassell MD. Cortical, thalamic, and amygdaloid connections of the anterior and posterior insular cortices. J. Comp. Neurol 1998;399:440–468. [PubMed: 9741477]

Shigemoto R, Nakanishi S, Mizuno N. Distribution of the mRNA for a metabotropic glutamate receptor (mGluR1) in the central nervous system: an in situ hybridization study in adult and developing rat. J. Comp. Neurol 1992;322:121–135. [PubMed: 1430307]

Shigemoto R, Nomura S, Ohishi H, Sugihara H, Nakanishi S, Mizuno N. Immunohistochemical localization of a metabotropic glutamate receptor, mGluR5, in the rat brain. Neurosci. Lett 1993;163:53–57. [PubMed: 8295733]

Sun N, Cassell MD. Intrinsic GABAergic Neurons in the Rat Central Extended Amygdala. J. Comp. Neurol 1993;330:381–404. [PubMed: 8385679]

Testa CM, Friberg IK, Weiss SW, Standaert DG. Immunohistochemical localization of metabotropic glutamate receptors mGluR1a and mGluR2/3 in the rat basal ganglia. J. Comp. Neurol 1998;390:5–19. [PubMed: 9456172]

Tsvetkov E, Carlezon WA, Benes FM, Kandel ER, Bolshakov VY. Fear conditioning occludes LTP-induced presynaptic enhancement of synaptic transmission in the cortical pathway to the lateral amygdala. Neuron 2002;34:289–300. [PubMed: 11970870]

Valenti O, Conn PJ, Marino MJ. Distinct physiological roles of the Gq-coupled metabotropic glutamate receptors Co-expressed in the same neuronal populations. J. Cell Physiol 2002;191:125–137. [PubMed: 12064455]

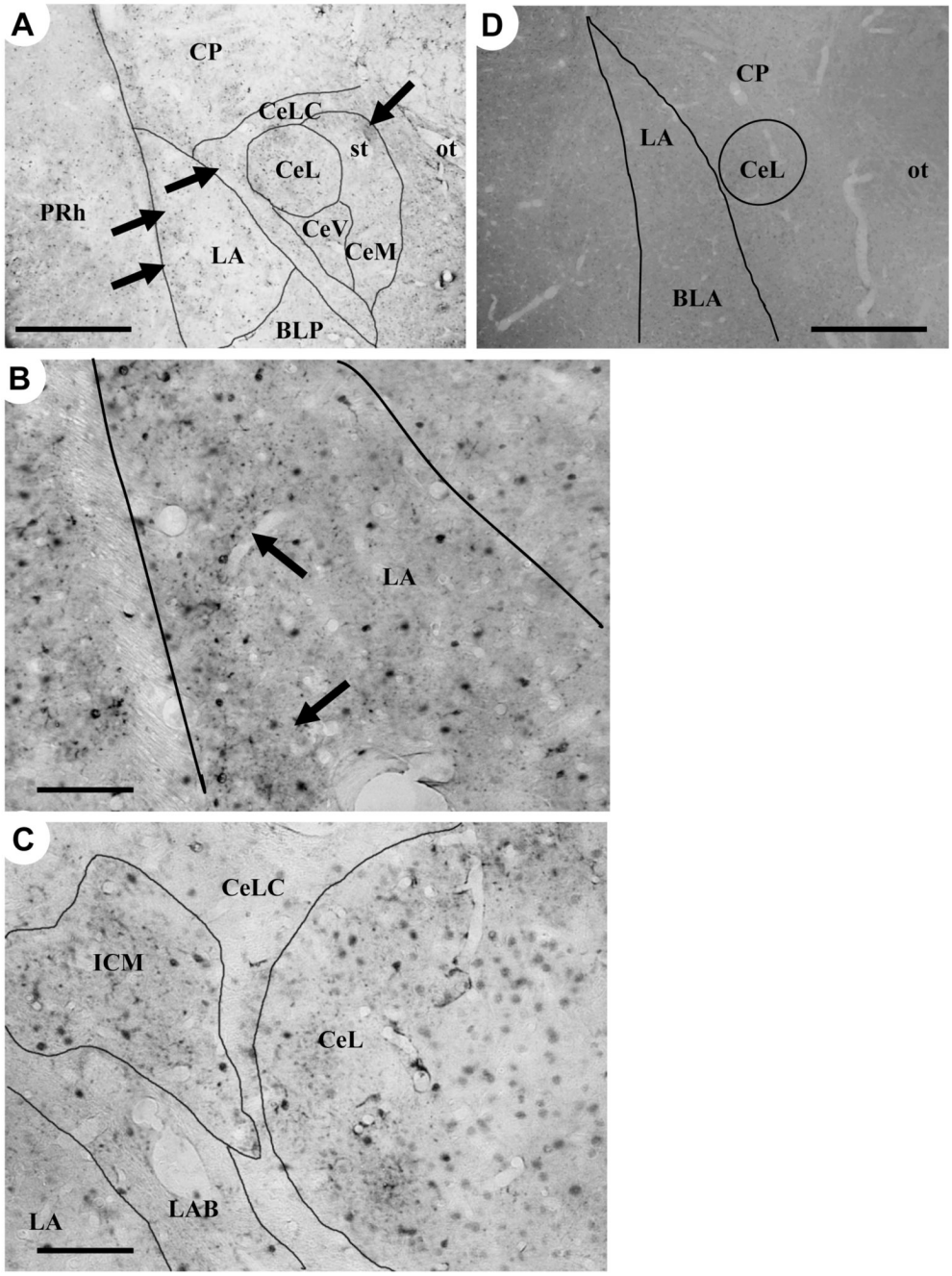

Fig.1.

A - Coronal section (40μM thick) through roughly the mid-rostrocaudal level of the amygdala processed for caldesmon immunohistochemistry. Arrows point to intercalated cell masses (ICM) identified from counterstained sections.

B - High power micrograph of lateral nucleus of the amygdala (LA). Note the scattered distribution of Cd-immunoreactive cells and the patches of punctate staining (arrows) along its lateral edge.

C – High power micrograph of the dorsolateral part of the central amygdaloid nucleus showing ICM with punctate staining and Cd-immunopositive neurons in the ICM and lateral CE division (CeL).

D – Section through the amygdala following immunocytochemistry with the anti-caldesmon antibody preadsorbed with the immunizing peptide. Note the complete abolition of immunostaining. BLA – anterior division of basolateral nucleus; BLP – posterior division of basolateral nucleus; CE - central nucleus of amygdala; CeM – medial subdivision of CE; CeL – lateral subdivision of CE; CeLC – lateral capsular division of CE; CeV – ventral subdivision of CE; CP – caudate-putamen; LA-lateral nucleus of amygdala; LAB – longitudinal association bundle; ICM - intercalated cell mass; PRh – perirhinal cortex; st – stria terminalis; ot – optic tract.. Scale bars in **A** and **D** – 0.5 mm; in **B** and **C** – 0.2 mm.

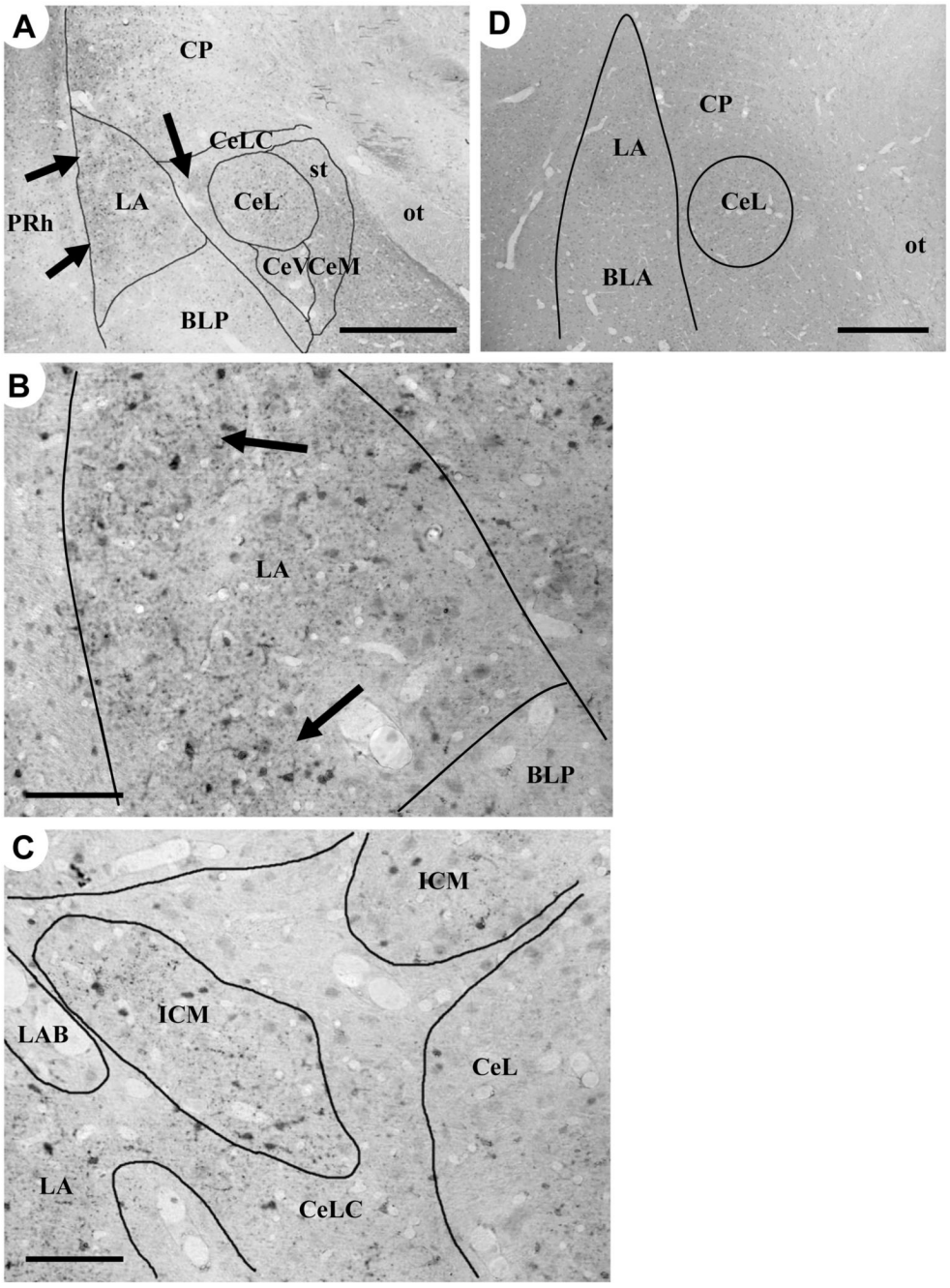

Fig. 2.

A - Coronal section of amygdala processed for calponin immunohistochemistry. Arrows point to location of ICM.

B – High power micrograph of Cp immunoreactivity in the lateral nucleus. Note patches of punctate staining and immuno-positive neurons (arrows).

C - High power view of the dorsolateral corner of the central nucleus of the amygdala showing patches of punctate staining in the ICM as well as Cp immunopositive neurons there and in the lateral central nucleus (CeL).

D – Section through amygdala following immunocytochemistry where the primary antibody directed against Cp was pre-adsorbed with the immunizing peptide.

Abbreviation and scale bar as on Fig. 1.

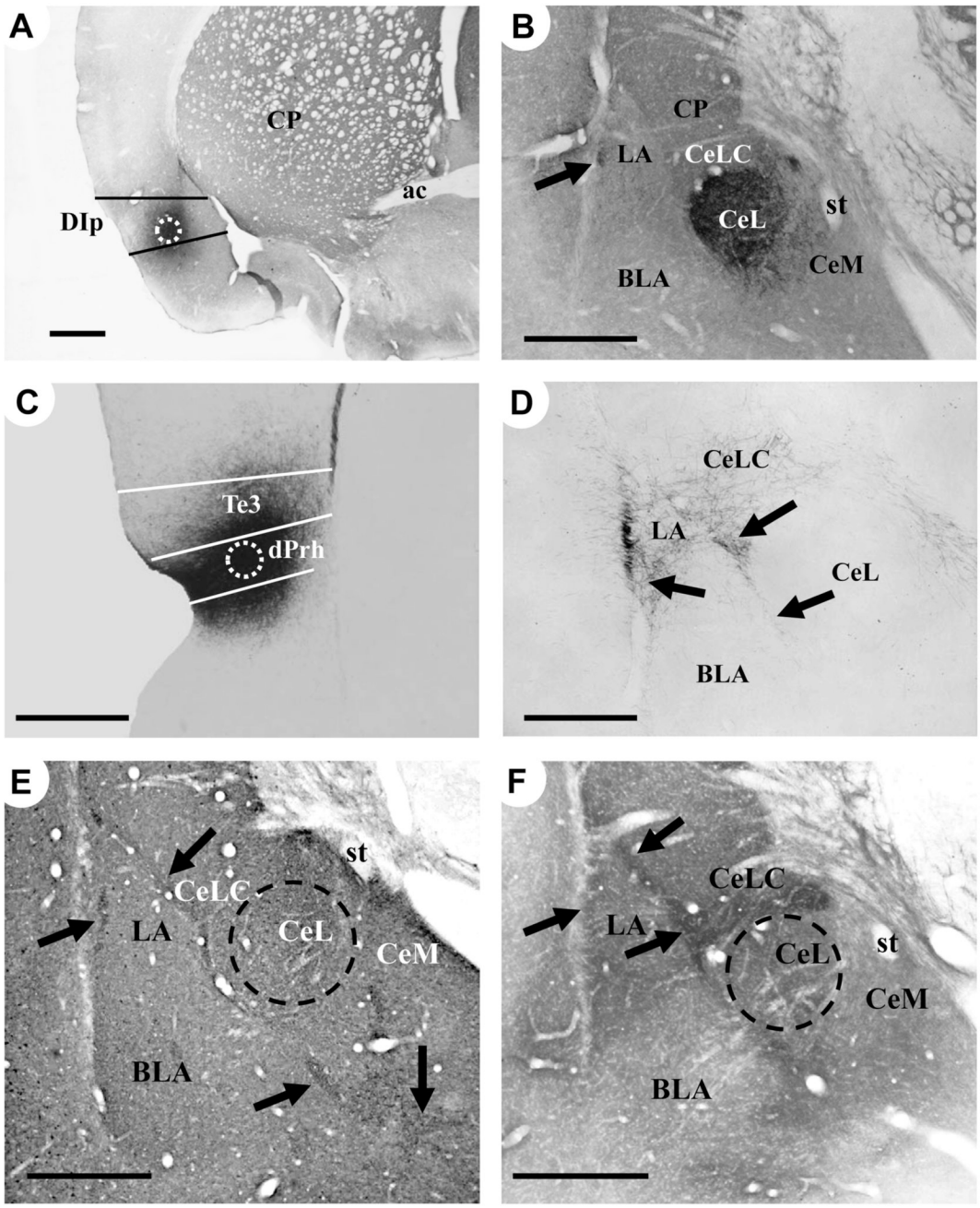

Fig. 3.

A – Location of representative BDA injection site (white dots show center) made in the posterior dysgranular insular cortex (DIp) at roughly the level of bregma.

B – Coronal section (50μM thick) through the dorsal amygdala showing distribution of BDA labeled fibers and terminals (black punctate staining) following DIp injection (panel **A**). Axons and terminals are confined to the lateral central nucleus (CeL) and dorsolateral edge of the lateral nucleus (arrow).

C – Location of representative BDA injection site (white dots) in the dorsal perirhinal cortex (dPRh). Te3- temporal association cortex;

D – Coronal section (50μM thick) through dorsal amygdala showing BDA labeled axons and terminals in the lateral nucleus and dorsal part of the lateral capsular division of the CE (CeLC). Following injection into dPRh (e.g. panel C). Arrows point to the location of ICM.
E – Coronal section (30μM thick) through the dorsal amygdala processed for mGluR1α immunohistochemistry. Note the concentration of the punctate immunoreactivity in the ICM (arrows) and CeL. Cell body labeling is also evident in these areas.
F – Coronal section (50μM thick) through the dorsal amygdala processed for mGluR5 immunohistochemistry. While the overall distribution pattern is similar to that for mGluR1α, particularly in the ICM (arrows), note the greater density of immunoreactivity in the dorsal CE.
All scale bars: 0.5 mm.

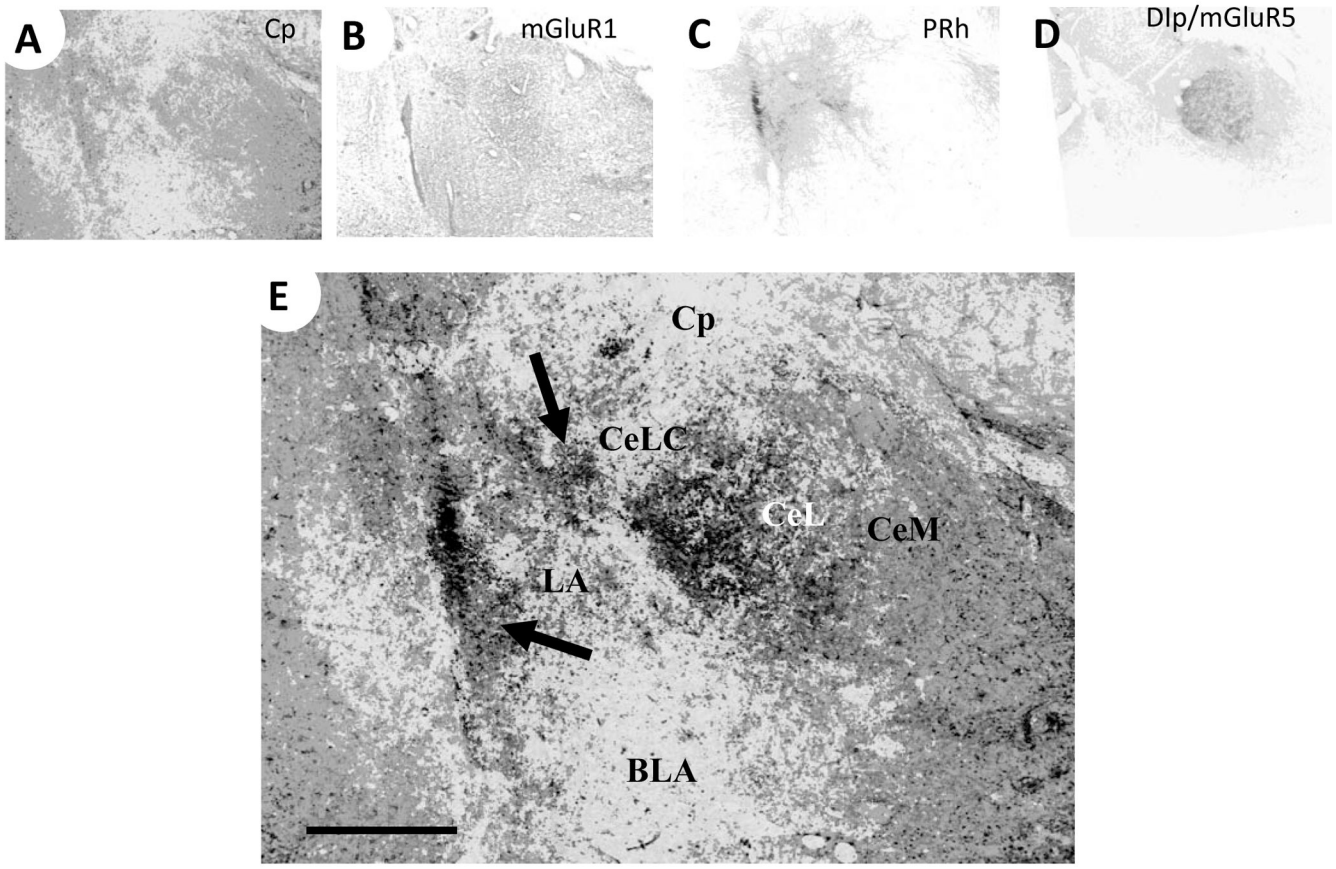

Fig. 4.

A – D. Gray scale renderings of the amygdala distribution and relative density of immunostaining for caldesmon (A) and mGluR1α (B), and axon terminals from the dPRh (C), and axon terminals from posterior dysgranular insular cortex (DIp) combined with mGluR5 immunostaining (D). In each of these images, the densest labeling was given a gray value of 64 and the absence of labeling a value of 0. Density differences were partitioned into eight different levels.

E – Merged composite of panels A–D. Here, the greatest area of overlap is rendered black while the area of least overlap is rendered white. Note the areas of greatest overlap of caldesmon, mGluR1α and cortical inputs are in the ICM in the LA and CeLC (arrows) and CeL.

Abbreviations as on Fig. 1; scale bar: 0.5 mm.

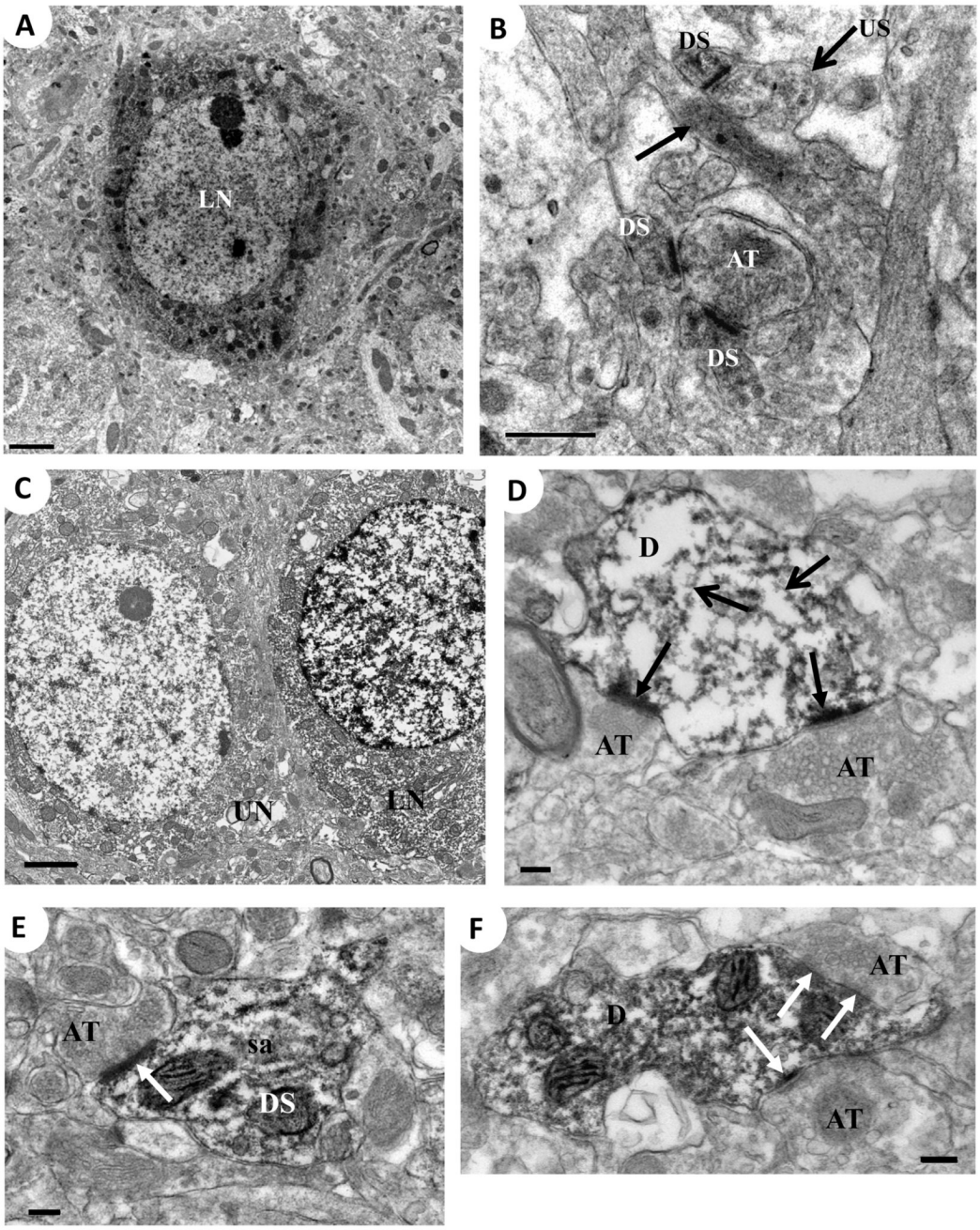

Fig. 5. Ultrastructural localization of caldesmon in the amygdala

A - An immunopositive neuron (LN) in LA showing Cd IR in its cytoplasm and, to a lesser extent, nucleus.

B - Three Cd-immunoreactive dendritic spines (DS) in LA synapsing with unlabeled axon terminals (AT). Note at top right the unlabeled dendritic spine (US) adjacent to the labeled spine and the presence of Cd-IR in the adjacent part of the parent dendrite (arrow).

C – A typical immunopositive neuron in the CE (LN) showing Cd IR in its cytoplasm and nucleus. Note the adjacent immunonegative neuron (UN).

D – A Cd-immunopositive dendrite in CE making asymmetric synaptic contacts with two different axon terminals. Note the strong accumulation of reaction product in the post-synaptic densities (solid arrows) and that associated with microtubules (open head arrows).
E – A Cd-immunopositive dendritic spine (note spine apparatus –sa) in CE making an asymmetric synapse with an axon terminal. A strong accumulation of reaction product in the PSD (arrow) is evident.
F – A Cd-immunopositive dendrite in CE contacted by two different axon terminals making symmetric synapses (arrows).
Scale bars: 2.0 μm for **A**; 0.2 μm for **B–D**; 0.5 μm for **E**.

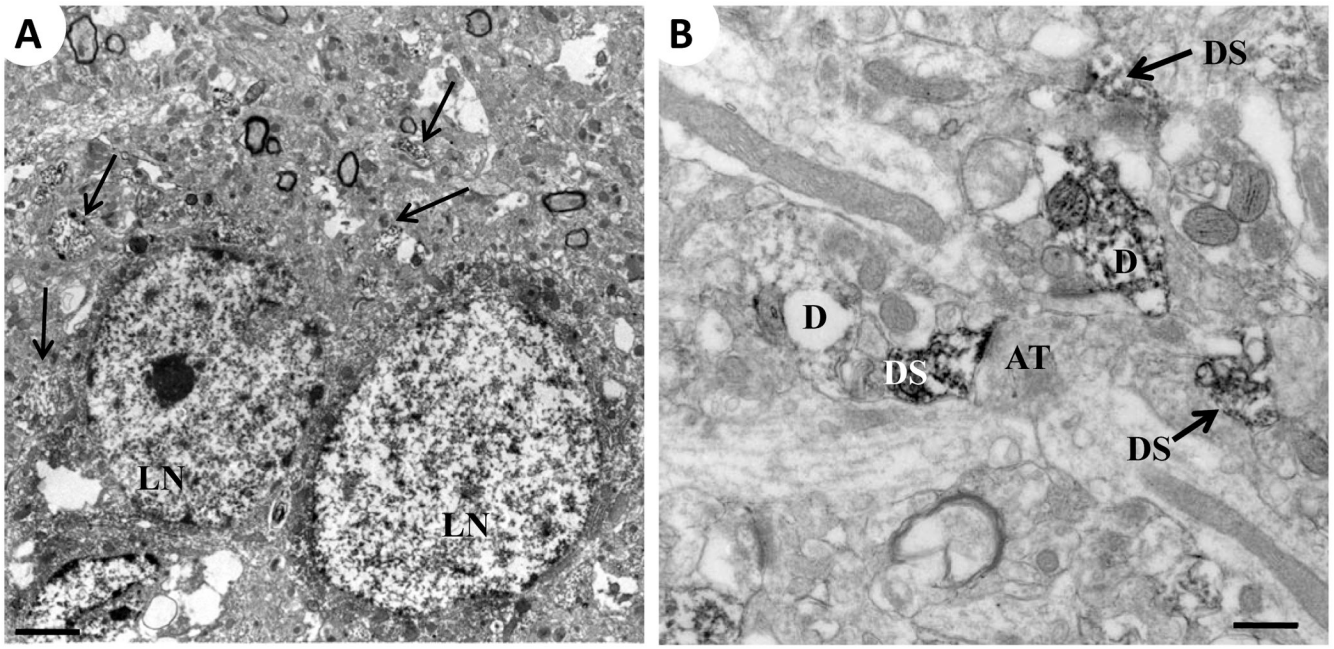

Fig. 6. Ultrastructural localization of Cp in the lateral nucleus

A - Two Cp-immunopositive neurons in LA showing Cp IR in their cytoplasm and nuclei. Note the relative scarcity of dendritic labeling (arrows).

B - Three Cp-immunoreactive dendritic spines (DS) in the LA. Note the very sparse distribution of immunoreactivity in dendrites (D) but heavy accumulation in spines.

Abbreviations as on Fig. 5. Scale bars: 2.0μm for **A**; 0.5 μm for **B**.

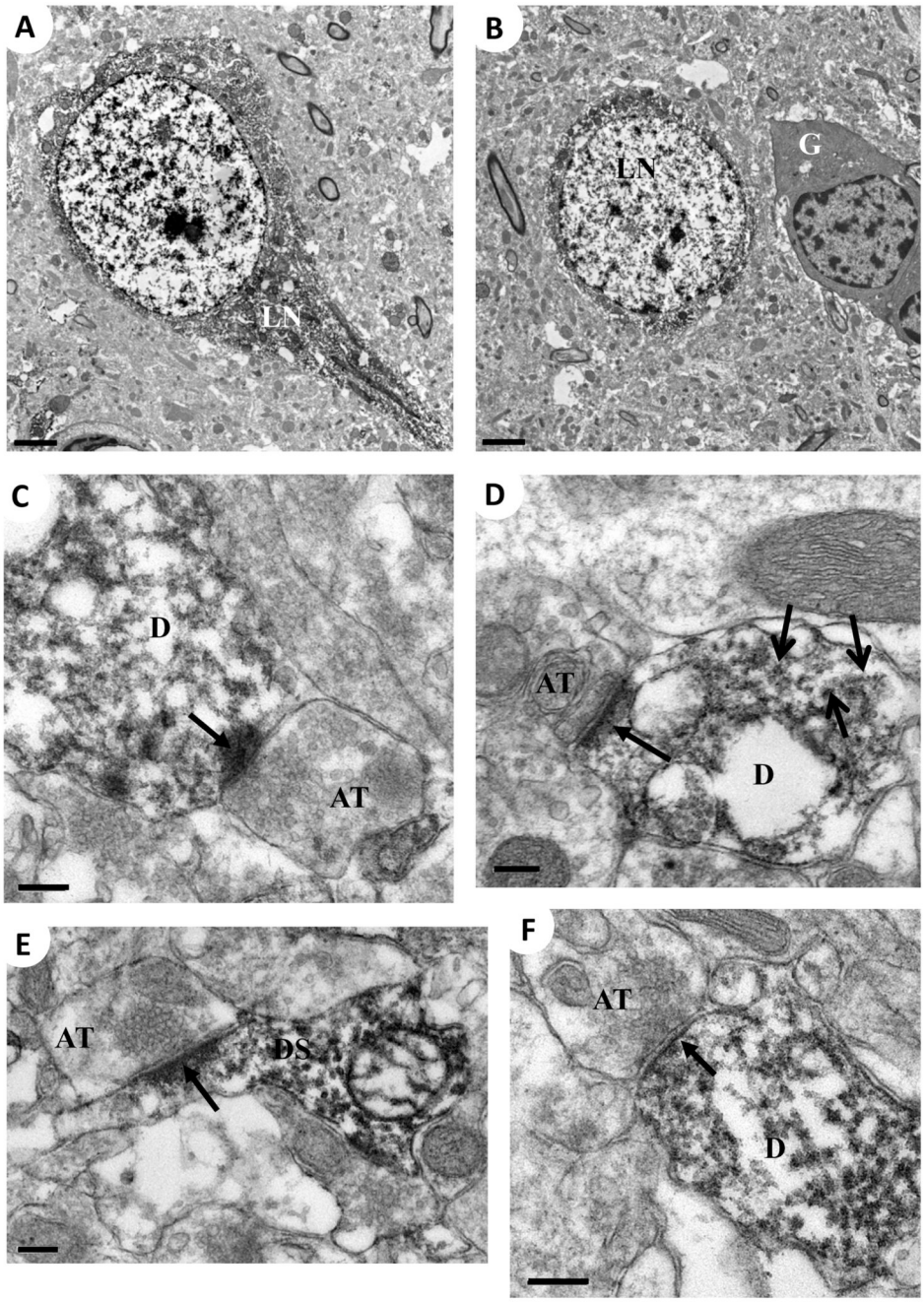

Fig.7. Cellular distribution of calponin immunoreactivity in the central nucleus

A – A typical Cp-immunopositive neuron with Cp-IR in its cytoplasm, nucleus and the proximal part of a dendrite.

B – No Cd or Cp immunoreactivity was identified in glia in the amygdala. Here a Cp-immunopositive neuron lies adjacent to an unlabelled glial cell.

C – A Cp-immunopositive dendrite in CE forming an asymmetric synapse with an axon terminal. As with caldesmon, there is a strong accumulation of reaction product in the PSD (arrow).

D – A Cp- immunopositive dendrite showing strong accumulation of Cp IR associated with microtubules (open head arrows) and PSD (solid arrow).

E – A Cp-immunopositive dendritic spine forms an asymmetric synapse with an axon terminal (arrow). This was the commonest type of Cp-immunoreactive structure identified ultrastructurally.

F – Rarely, a Cp-immunopositive dendrite was observed making a symmetric synapse with an axon terminal. A modest accumulation of reaction product along the postsynaptic membrane (arrow) is evident.

Abbreviations as on Fig. 5. Scale bars: 2.0 μm for **A–B**; 0.2 μm for **C–F**.

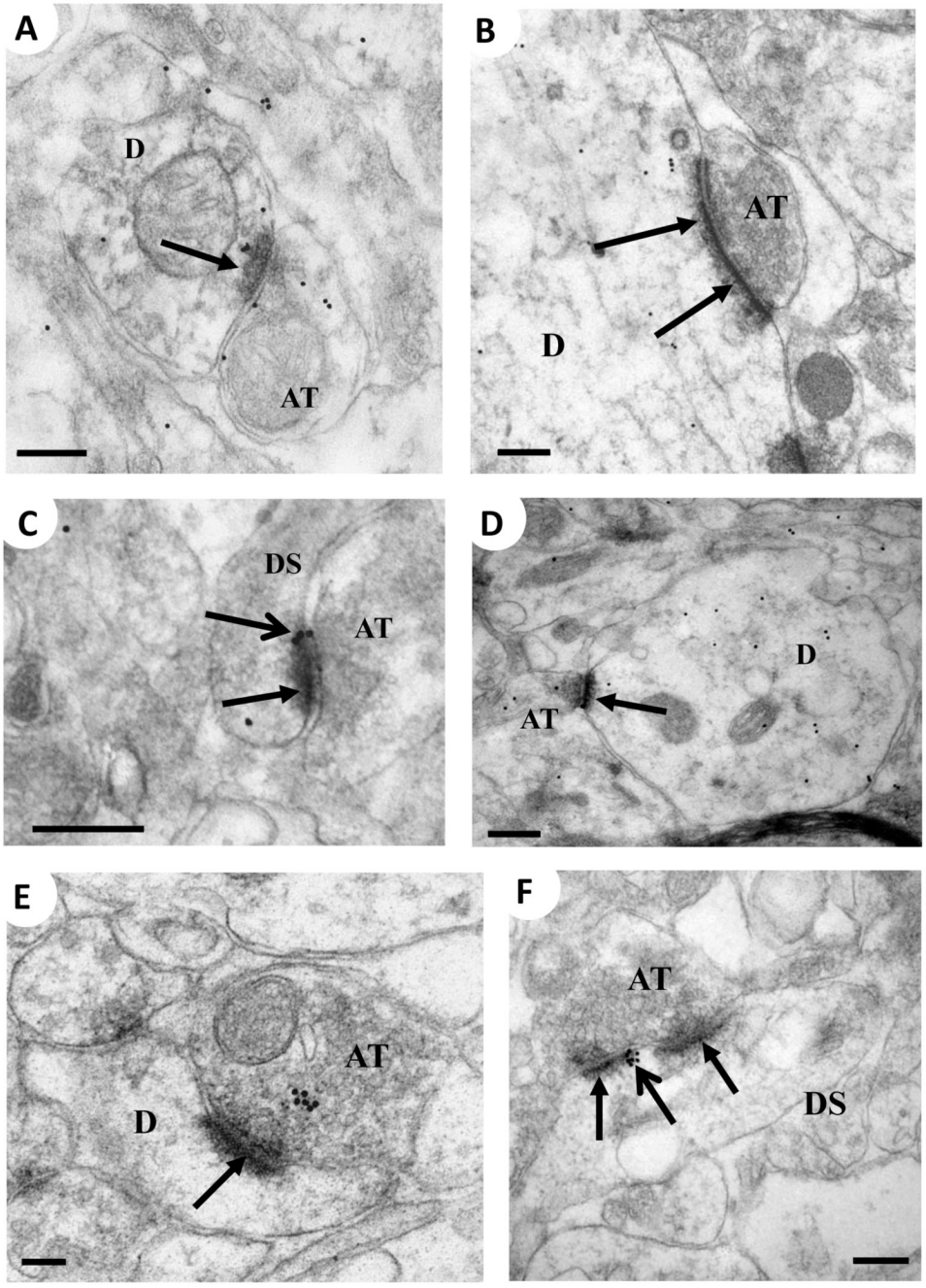

Fig. 8. Caldesmon and calponin immunocytochemistry in the CE combined with TrkB post-embedding immunogold staining (black dots). Note that the electron micrographs containing gold particles in this and other plates were printed with a lower contrast to give the particles better visibility

A – Cd and TrkB-positive dendrite with strong Cd IR in PSD (arrow) making an asymmetric synapse with a TrkB-positive axon terminal.

B – A TrkB-positive dendrite with dense accumulation of Cd IR in PSD (arrows) forms an asymmetric synapse with a TrkB-negative axon terminal. Gold particles can be observed on and around the PSD. This was the commonest type of labeling pattern seen in this material.

C – Dendritic spine (DS) with accumulation of Cd (solid arrow) and TrkB in PSD (open head arrow).
D – TrkB-positive dendrite with Cp IR associated with a PSD (arrow) making an asymmetric synapse with a TrkB-positive axon terminal.
E – TrkB-negative dendrite (possibly a spine) with strong Cp IR at a PSD (arrow) making an asymmetric synapse with a TrkB-positive axon terminal.
F – Dendritic spine with strong TrkB IR (open head arrow) and Cp IR (solid arrows) in PSDs making two asymmetric synapses with an axon terminal (AT).
Abbreviations as per Fig. 5. Scale bars: 0.2 μm for **A–C** and **F**; 0.1 μm for **E**.

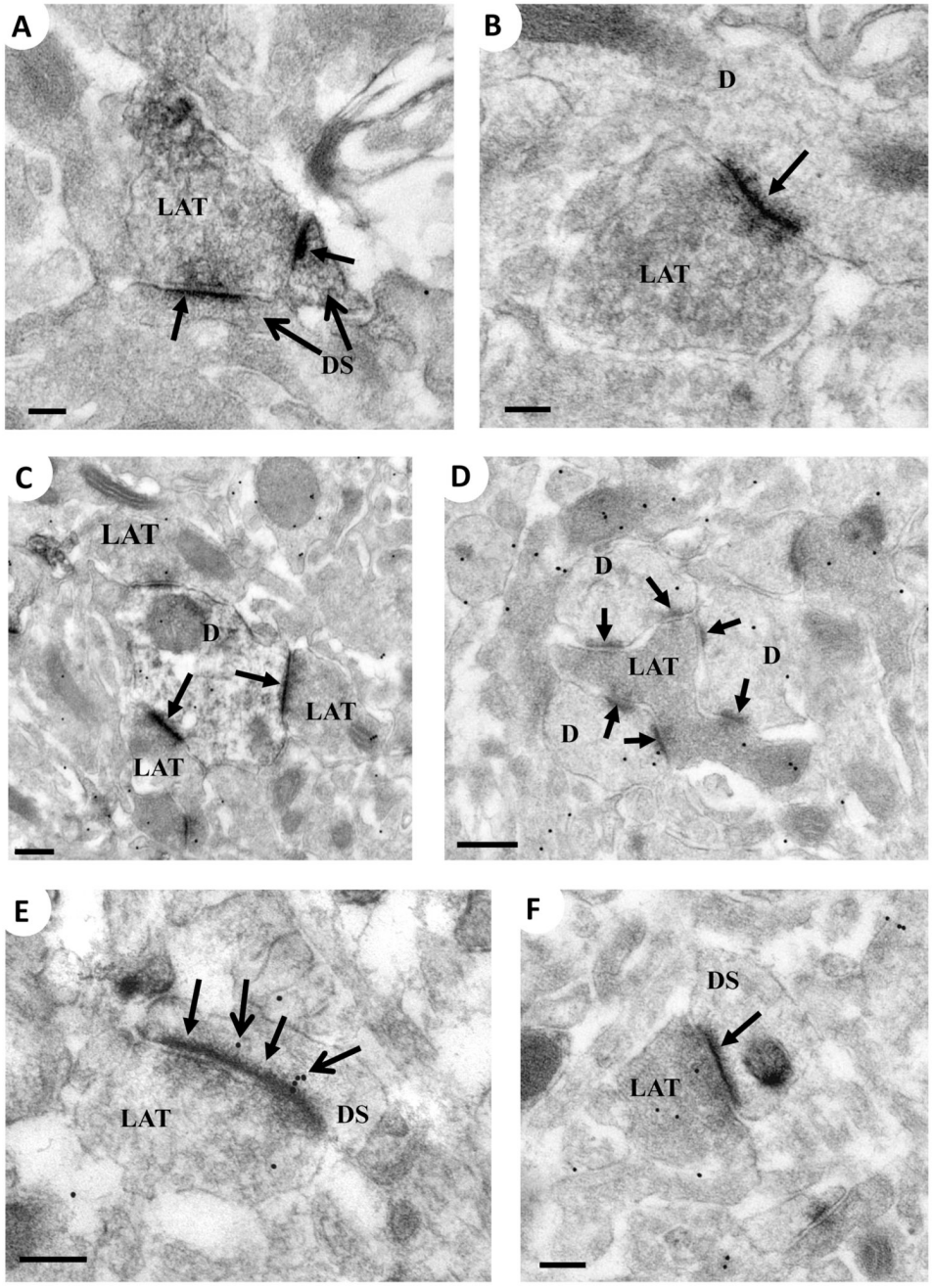

Fig.9. Interactions between mGluR1s, cortical terminals and TrkB receptors in the CE

A – A BDA-labeled (insular) cortical terminal (LAT) forming asymmetric synapses with two mGluR1α-positive dendritic spines (DS). Note strong association of mGluR1α immunoreactivity with PSDs (arrowheads).

B – A BDA-labeled cortical terminal (LAT) forming an asymmetric synaptic contact with a dendrite showing mGluR1α IR at a PSD (arrowhead).

C – A TrkB-positive dendrite (gold particles) with mGluR1α immunoreactivity in PSDs (arrows) forms synaptic contacts with two BDA-labeled cortical terminals (LAT) and one unlabelled terminal (AT). These contacts all appear to be of the asymmetric type.

D – TrkB-positive (note gold particles) and BDA-labeled cortical terminal (LAT) making contact with three dendrites having mGluR1α IR in PSDs (arrows). One of the dendrites is also TrkB-positive.

E and F – BDA-labeled cortical terminals (LAT) forming contacts with mGluR1 immunoreactive dendritic spines (DS). In E, there is TrkB immunoreactivity (gold particles) associated with the PSD while in **F**, gold particles are associated with the cortical terminal. Abbreviations as on Fig. 5. Scale bars: 0.1 μm for **A**, 0.2 μm for **B–F**.

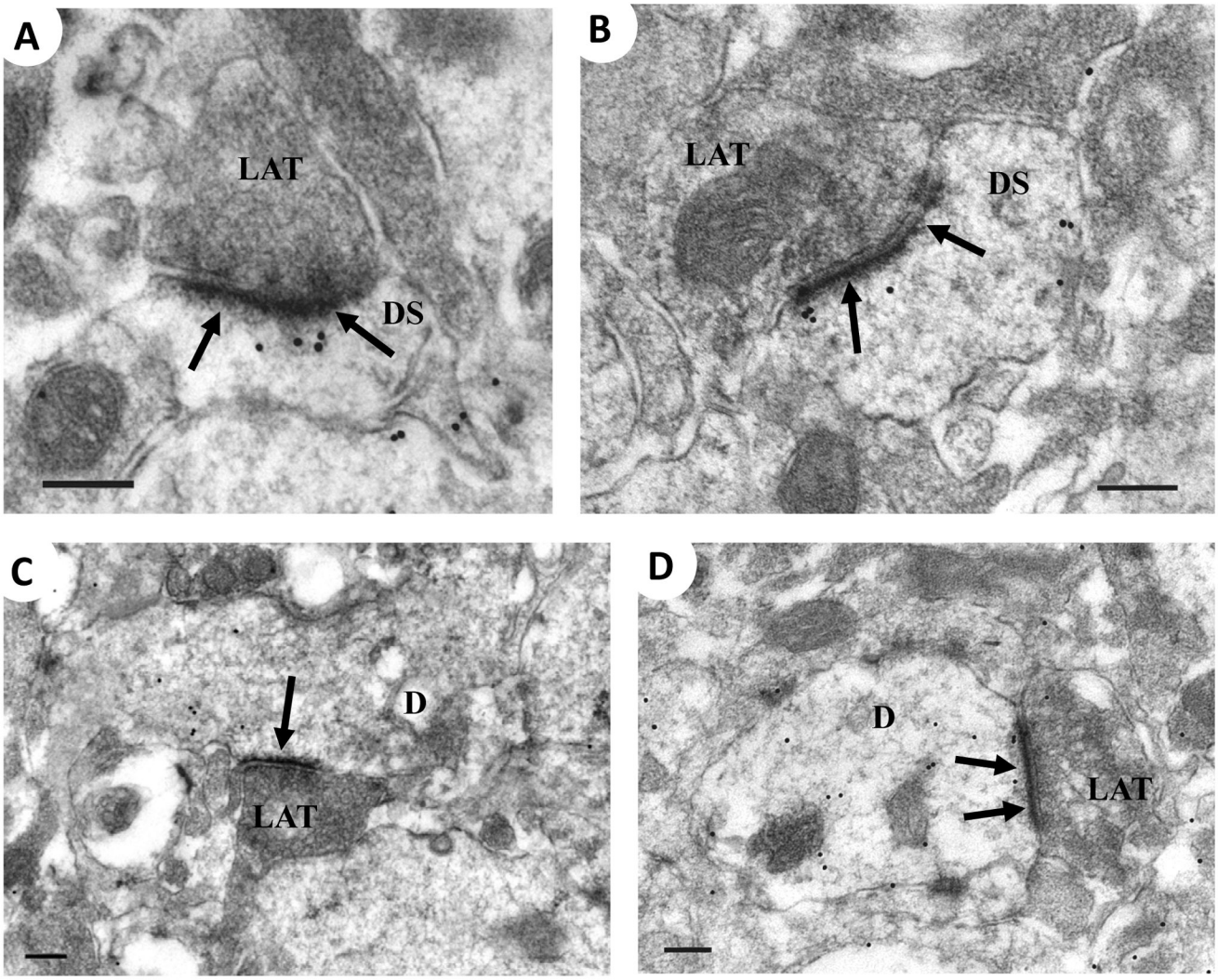

Fig. 10. Caldesmon and calponin post-embedding immunocytochemistry using gold particles (black dots) in the CE combined with pre-embedding mGluR5 staining and BDA labeling of cortical terminals

A – A Cd-positive dendritic spine with strong mGluR5 IR in PSD (arrows) making an asymmetric synapse with a BDA labeled cortical axon terminal.

B – A Cp-positive dendritic spine with strong mGluR5 IR in PSD (arrows) making an asymmetric synapse with a BDA labeled cortical axon terminal.

C - A Cd-positive dendrite with strong mGluR5 IR in PSD (arrow) making an asymmetric synapse with a BDA labeled cortical axon terminal.

D - A Cp-positive dendrite with strong mGluR5 IR in PSD (arrows) making an asymmetric synapse with a BDA labeled cortical axon terminal.

Abbreviations as per Fig. 5. Scale bars: 0.2 μm for **A–C**.